

J. MIAO<sup>1,2,✉</sup>  
B. WANG<sup>1,2</sup>  
J. PENG<sup>1,2</sup>  
H. TAN<sup>1</sup>  
H. BIAN<sup>1,2</sup>

# Highly stable and efficient KTP-based intracavity optical parametric oscillator with a diode-pumped passively Q-switched laser

<sup>1</sup> Changchun Institute of Optics, Fine Mechanics and Physics, Chinese Academy of Sciences, Changchun, Jilin 130033, P.R. China

<sup>2</sup> Graduate School of Chinese Academy of Sciences, Beijing 100039, P.R. China

Received: 22 January 2007/Revised version: 25 April 2007  
Published online: 16 June 2007 • © Springer-Verlag 2007

**ABSTRACT** We present in this paper a highly stable and efficient KTP-based intracavity optical parametric oscillator with a diode-end-pumped Nd:YVO<sub>4</sub>/Cr:YAG passively Q-switched laser. At the incident diode pump power of 4 W, the signal (1.57 μm) and idler (3.29 μm) average output powers up to 580 and 100 mW, respectively, have been achieved. The corresponding conversion efficiency from the input diode pump power to the output signal power is 14.5%, while that to the total OPO output (signal + idler) reaches 17%. To the best of our knowledge, these are the highest conversion efficiencies reported to date. After more than four hours of investigation, the OPO power stability better than 2% has been obtained. In addition, efficient cavity dumping of the IOPO has inevitably led to the short pulse duration (1.6 ns) and high peak power output (8.3 kW) at the signal wave. Additionally, the amplitude and repetition rate fluctuations of the signal pulses are well within 5%.

PACS 42.55.Xi; 42.60.Gd; 42.60.Lh; 42.65.Yj

## 1 Introduction

In recent years, more and more extensive attentions have been paid to research on intracavity optical parametric oscillators (IOPO). Compared with the extracavity OPO (EOPO), IOPO possesses several distinct merits such as compactness, low threshold, high efficiency, etc. The main idea of the IOPO is to take advantage of the high fundamental intensity within the pump laser cavity [1]. Thus, the pump level necessary to exceed the OPO threshold is greatly reduced even in the case of single resonant OPO, and the parametric conversion efficiency is inevitably enhanced. Actually, IOPO acts very like a cavity dumper to fully and rapidly extract the pump energy into the signal and idler fields.

IOPO was first experimentally accomplished by Ammann et al. more than 30 years ago [2]. However, owing to the lack of nonlinear crystals with high damage threshold and large effective nonlinear coefficient, research in this field was neglected until the early 1990s when high quality nonlinear optical materials such as LBO, BBO, KTP, etc., were developed [3]. Since then, studies on the KTP-based IOPO

emitting at 1.5 μm eye-safe wavelength became a new and promising branch in the field of optical parametric oscillators. Nevertheless, at that period the pump sources mainly were flash-lamp or quasi-cw diode side-pumped actively Q-switched Nd:YAG lasers [4, 5], with low pulse repetition rate and low conversion efficiency.

High repetition rate pulsed laser radiations around 1.5 μm are indispensable for applications such as laser radar, remote sensing, etc. To achieve this, a cw diode-end-pumping scheme is often required [6]. Compared with Nd:YAG, the main superiority of the Nd:YVO<sub>4</sub> crystal lies in its linearly polarized output characteristic, which is preferable not only for nonlinear frequency conversion, but also for the elimination of the undesired birefringent effects [7]. In addition, the recently developed Cr:YAG passively Q-switched lasers, with the benefits of low cost, high efficiency, compactness and simplicity [8, 9], have become an alternative to actively Q-switched lasers. Therefore, cw diode-end-pumped Nd:YVO<sub>4</sub>/Cr:YAG passively Q-switched lasers should be the ideal pump sources for the IOPO. The first KTP-based IOPO driven by the laser source similar to that mentioned above was realized by Conroy et al. [10]. Since the early 2000s, Chen [11, 12] and Zendjian [6] demonstrated several such IOPOs with 1.5 μm eye-safe signal output. However, the diode to signal conversion efficiencies were limited within 11%. No attempt has been made to discuss the pulse and power stabilities of the IOPO. Moreover, for the severe absorption at wavelengths longer than 3.1 μm in KTP, the idler (3.29 μm) behavior of the KTP-based IOPO has seldom been discussed except for the works reported by Kato [13] and Dubois et al. [14].

In this report, we demonstrate a highly stable and efficient KTP-based optical parametric oscillator intracavity pumped by a Nd:YVO<sub>4</sub>/Cr:YAG passively Q-switched laser. With the idler field being coupled out of the OPO cavity, the conversion efficiency from the input diode pump power to the total OPO outputs (signal + idler) is as high as 17%. To the best of our knowledge, this is higher than any other previous work reported to date. Moreover, the OPO pulse and power stabilities better than 5% and 2%, respectively, have been achieved.

## 2 Experimental setup

The elaborate design of the compact IOPO system is schematically shown in Fig. 1. A passively Q-switched Nd:YVO<sub>4</sub>/Cr:YAG laser, longitudinally driven by a 5 W cw

✉ Fax: +86-431-85604748, E-mail: mjgbhk@yahoo.com

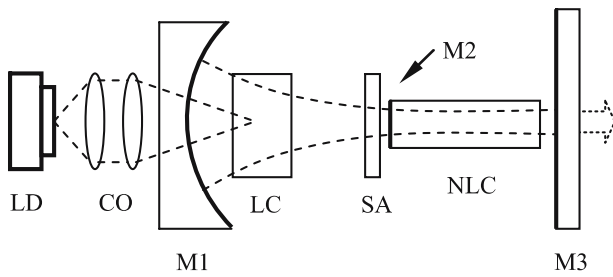


**FIGURE 1** Experimental setup of the IOPO system. LD laser diode. CO coupling optics. M1 input mirror. LC laser crystal. SA Cr:YAG saturable absorber. NLC KTP crystal. M3 output coupler

diode laser (806.5 nm, Lasertel LT-1030), was employed as the pump source of the OPO. In order to enhance the parametric gain and reduce the OPO threshold, a plane-concave cavity configuration was used in this setup to set the pump beam waist near the KTP crystal. For the divergent and unsymmetrical emitting property of the diode, a well designed coupling optics was used here, with a coupling efficiency of 93%. With the benefits of broad absorption bandwidth and linearly polarized emitting property, a  $3 \times 3 \times 5 \text{ mm}^3$ , *a*-cut, 0.5 at. % doped Nd:YVO<sub>4</sub> crystal was used as the active medium which was anti-reflection (AR) coated at 1064 nm on both sides. The Cr:YAG saturable absorber, with an initial transmission of 83% and a thickness of 1.8 mm, was also AR coated at the fundamental wave on the two end faces. A 20 mm long, type-II noncritically phased-matched ( $\theta = 90^\circ$ ,  $\varphi = 0^\circ$ ) KTP crystal was used in the experiment as the nonlinear parametric converter. Moreover, for the purpose of reducing the inserting loss, one side of the KTP was coated as one of the OPO cavity mirrors (M2), which was high transmission (HT) coated at 1064 nm ( $T > 98\%$ ), high reflection (HR) coated at 1573 nm ( $R > 99.8\%$ ), and was AR coated at the two wavelengths on the other side. As the input mirror, M1 was highly transmitting at 808 nm on both sides and highly reflecting at 1064 nm on the concave one, with a radius of curvature of 50 mm. Serving as the cavity mirrors for both the fundamental and the OPO cavities, M3 was HR coated at 1064 nm ( $R > 99.8\%$ ), HT at 3288 nm ( $T > 90\%$ ) and partly reflecting at 1573 nm ( $R = 92\%$ ) on one side, and was AR coated at the signal (1.57  $\mu\text{m}$ ) and idler (3.29  $\mu\text{m}$ ) waves on the other side. In order to investigate the lasing behavior of the idler, a CaF<sub>2</sub> window material was employed as the substrate of M3. In addition, several thermo-electric coolers were used in the experiment to thermally stabilize the laser rod, Cr:YAG and KTP crystals.

### 3 Experimental results and discussion

To optimize the mode-to-pump ratio, the overall physical cavity length of the fundamental laser was determined to be around 58 mm, and that of the OPO (formed by M2 and M3) was as short as 22 mm. The diode pump light, through the coupling optics, was focused into the laser rod with a spot radius of about 100  $\mu\text{m}$ . Considering the strong absorption of the idler radiation in KTP, the present IOPO was designed to be single resonant at the signal wave. Anyhow, with the intention of observing the lasing behavior of the idler, we strove to couple this optical field outside the OPO cavity

through the CaF<sub>2</sub> window, which we assume was beneficial to improve the signal performance. Moreover, it is worthwhile to mention that since the emission cross section of the *a*-cut Nd:YVO<sub>4</sub> crystal is generally larger than the absorption cross section of the Cr:YAG saturable absorber, difficulties usually arise in the operation of diode-pumped Nd:YVO<sub>4</sub>/Cr:YAG passively Q-switched lasers. To achieve a good passive Q-switching, efforts, such as inserting a focusing lens into the cavity [15], optimizing the cavity design, etc., should be made to ensure a small mode area in the Cr:YAG crystal and further to match the second threshold criterion which is defined by [16]:

$$\frac{\ln(1/T_0^2)}{\ln(1/T_0^2) + \ln(1/R) + \delta} \frac{\sigma_{gs} A}{\sigma A_s} > \frac{\gamma}{1 - \beta} \quad (1)$$

where  $T_0$  and  $\sigma_{gs}$ , respectively, are the initial transmission and ground-state absorption cross section of the saturable absorber,  $R$  is the fundamental reflectivity of the output coupler,  $\delta$  is the nonsaturable intracavity round-trip dissipative optical loss,  $A/A_s$  is the ratio of the mode area in the active medium and in the saturable absorber,  $\sigma$  is the stimulated emission cross section of the Nd:YVO<sub>4</sub> crystal,  $\gamma$  is the inversion reduction factor, and  $\beta$  is the ratio of excited-state and ground-state absorption cross sections of the Cr:YAG crystal. From (1), it can be found that when the active medium and saturable absorber are given,  $A/A_s$  becomes a vital factor that affects the passively Q-switched laser performance. In the present configuration, the fundamental beam radii in the Nd:YVO<sub>4</sub> and Cr:YAG crystals were calculated to be 229  $\mu\text{m}$  ( $w_{Nd}$ ) and 92  $\mu\text{m}$  ( $w_{Cr}$ ), respectively. Thus, we obtained  $A/A_s = (w_{Nd}/w_{Cr})^2 \approx 6.2$ , which could satisfy the second threshold criterion referred to above.

Figure 2 depicts the average output power of the IOPO with respect to the incident diode pump power. The parametric oscillation threshold, in terms of the diode pump power, was as low as 0.63 W. It can be seen that the OPO average output power increased proportionally to the pump level, and no thermal lensing induced power fall-off has been observed dur-

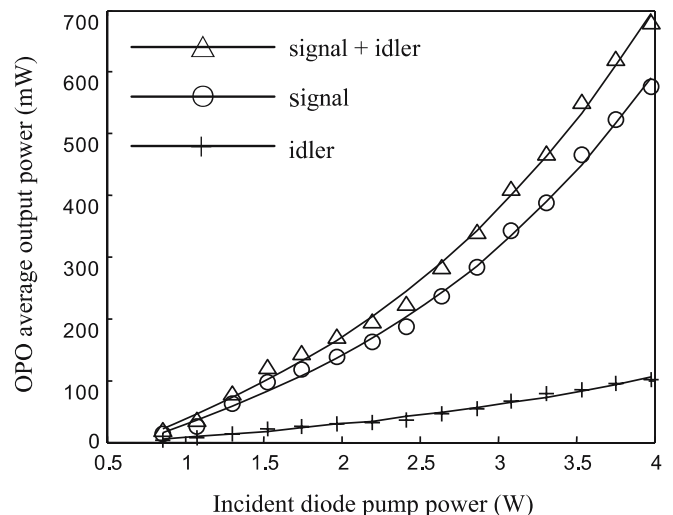


**FIGURE 2** High efficient average output power of the IOPO with respect to the incident diode pump power

ing the whole pump scope. At the diode pump power of 4 W, the total OPO average power (signal + idler) up to 680 mW has been achieved. In addition, by using a BK7 glass to block the idler, we obtained approximately 580 mW signal output in the experiment. Therefore, taking into account the gap between the signal and the total OPO outputs, the maximum average power at  $3.29 \mu\text{m}$  was indirectly found to be about 100 mW. Obviously, the idler output was only one-seventh of the total OPO output, which experimentally confirmed the idler-absorbing property of the KTP crystal. Furthermore, the conversion efficiencies from the input diode pump power to the signal and the total OPO outputs were calculated to be 14.5% and 17%, respectively. To the best of our knowledge, the conversion efficiencies mentioned above were higher than any other previous work reported to date. Basically, this can be attributed to the following two aspects. On the one hand,

with the idler energy being coupled out of the OPO cavity, absorbing at this wavelength in KTP was reduced, which simultaneously decreased the corresponding undesired thermal effects. On the other, owing to the depletion of the intracavity idler field, the parametric back conversion of the signal and idler radiations to that of the pump was weakened.

In order to accurately investigate the stability of the OPO output power, a computer program was employed to record and analyze the corresponding experimental data. At the maximal diode pump level, by recording the OPO output power per second, we have obtained more than four hours' power stability, pictured in Fig. 3. It is seen that the power fluctuation was better than 2% in the whole time range, exhibiting extremely stable OPO output. The far-field beam profile and spatial distribution of the signal radiation, detected by a Spiricon Laser Beam Diagnostics, were shown in Fig. 4. From this figure, one can see that the signal beam was near the diffraction limit and the laser intensities in the horizontal and vertical directions were ideally in the Gaussian distributions.

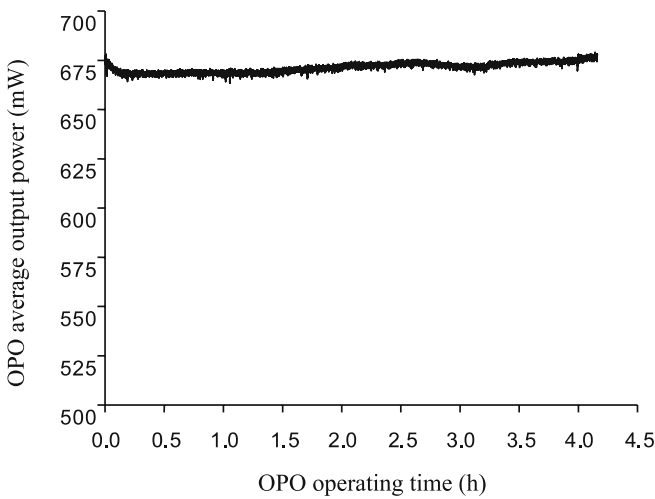


FIGURE 3 Long time stability of the OPO output power with fluctuations better than 2%

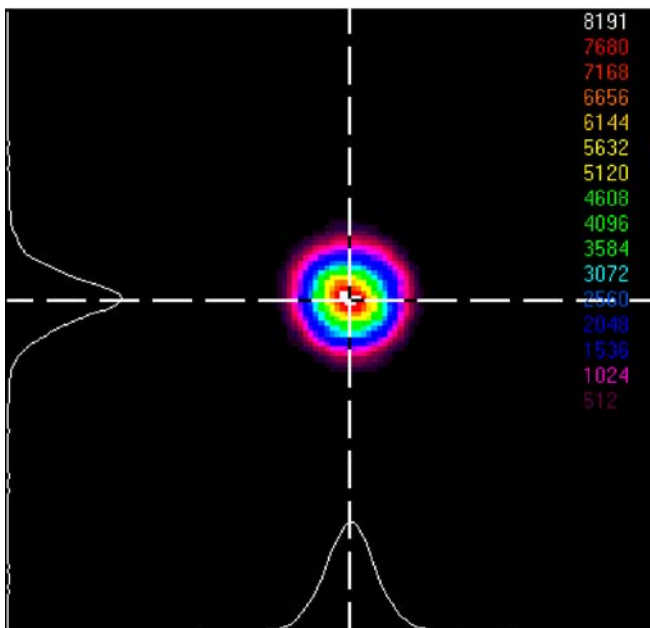


FIGURE 4 Diffraction limited far-field beam profile and intensity distributions of the signal wave

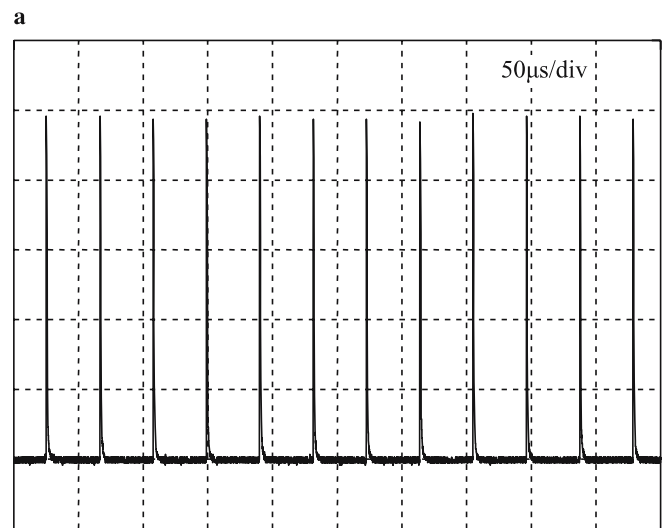


FIGURE 5 (a) Synchronous temporal profiles of the fundamental (curve 1) and signal (curve 2) pulses after the OPO began to oscillate. (b) A typical train of the pulses at  $1.57 \mu\text{m}$ , holding a pulse-to-pulse amplitude and repetition rate fluctuations within 5%

The temporal behaviors of the signal and fundamental pulses, detected by a fast InGaAs photodiode and recorded by a LeCroy9361C Dual 300 MHz oscilloscope, were illustrated in Fig. 5. In Fig. 5a are the synchronous temporal profiles of 1064 nm and 1573 nm pulses after the OPO began to oscillate. From it, one can see clearly the buildup mechanism of the signal pulses and also the correlation dynamics between the fundamental laser and the OPO, which have been discussed in detail in the previous published works [1, 17, 18]. In the experiment, we obtained a minimum signal pulse duration as short as 1.6 ns, which was about 13 times shorter than that of the fundamental wave (20 ns). Pulse shortening phenomenon is a typical characteristic of the IOPO, which can be interpreted as follows. It has been previously found that the signal pulse duration is close to the photon lifetime in the OPO cavity [1], and the general expression of the cavity photon lifetime can be defined by [19]:

$$\tau_j = \frac{2L_j}{c [\ln(1/R_j) + \delta_j]} \quad (2)$$

where  $j = s, p$  represents the signal and fundamental waves, respectively,  $L$  is the optical cavity length,  $c$  is the speed of light,  $R$  is the output reflectivity and  $\delta$  is the dissipative optical loss. In the case of IOPO, we surely have  $R_p > R_s$  and  $L_p > L_s$ . Hence, based on (2), one can easily discern that the signal photon lifetime is far smaller than that of the fundamental radiation. In other words, through the parametric conversion process, the signal pulses were compressed by several, even more than ten, orders of magnitude. In addition, highly stable trains of the signal pulses were experimentally observed at different pump levels. An oscilloscope trace of a sample train was recorded and plotted in Fig. 5b. As it shows, the pulse-to-pulse amplitude and repetition rate fluctuations were well within 5%. However, owing to the lack of appropriate detecting devices, we failed to observe the temporal behavior of the idler radiation under the present experimental conditions.

Figure 6 illustrates the pulse repetition rate and output peak power at 1.57  $\mu\text{m}$  as a function of the incident diode

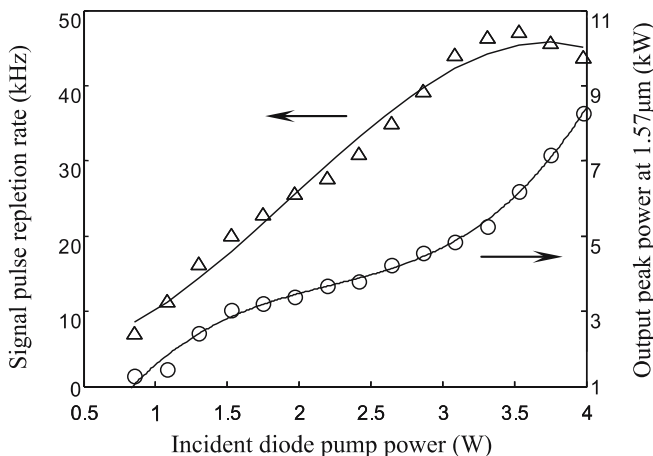


**FIGURE 6** Pulse repetition rate and output peak power at the signal wave as a function of the incident diode pump power

pump power. As it shows, the pulse repetition rate increased linearly with the pump level until the diode power went beyond 3.53 W where the repetition rate began to fall off from the maximal value of 47 kHz, owing to the thermal lens effects in the Nd:YVO<sub>4</sub> and Cr:YAG crystals. Besides, as mentioned in Sect. 1, cavity dumping is another typical property of the IOPO, which would lead to high peak power output at the parametric oscillating radiations. At the diode pump power of 4 W, as shown in Fig. 6, a signal peak power higher than 8.3 kW has been achieved.

#### 4 Conclusions

We have accomplished a compact highly stable and efficient KTP-based IOPO driven by a diode-end-pumped Nd:YVO<sub>4</sub>/Cr:YAG passively Q-switched laser. At the maximal diode pump level, the IOPO produced average output power as high as 680 mW, which comprises the contributions of 580 mW at 1.57  $\mu\text{m}$  and 100 mW at 3.29  $\mu\text{m}$ . The diode-to-signal and diode-to-OPO (signal + idler) conversion efficiencies up to 14.5% and 17%, respectively, have been obtained. As far as we know, these are the highest conversion efficiencies reported to date. Besides, the OPO power and pulse stabilities were found to be better than 2% and 5%, respectively. Experimental results indicated that decreasing the absorption at the idler radiation in KTP is beneficial to improving the OPO performance. The present device makes further progress into the commercialization and application of the KTP-based IOPO.

#### REFERENCES

- 1 T. Debuisschert, J. Raffy, J.-P. Pocholle, M. Papuchon, *J. Opt. Soc. Am. B* **13**, 1569 (1996)
- 2 E.O. Ammann, J.M. Yarborough, M.K. Oshman, P.C. Montgomery, *Appl. Phys. Lett.* **16**, 309 (1970)
- 3 L.R. Marshall, A. Kaz, R.L. Burnham, *Proc. SPIE* **1627**, 262 (1992)
- 4 E.V. Raevsky, V.L. Pavlovitch, V.A. Kononov, *Proc. SPIE* **4630**, 75 (2002)
- 5 R. Dabu, A. Stratan, C. Fenic, C. Luculescu, L. Muscalu, *Opt. Eng.* **40**, 455 (2001)
- 6 W. Zendzian, J.K. Jabczynski, P. Wachulak, J. Kwiatkowski, *Appl. Phys. B* **80**, 329 (2005)
- 7 Y.F. Chen, S.W. Chen, Y.C. Chen, Y.P. Lan, S.W. Tsai, *Appl. Phys. B* **77**, 493 (2003)
- 8 X. Zhang, S. Zhao, Q. Wang, Q. Zhang, L. Sun, S. Zhang, *IEEE J. Quantum Electron.* **QE-33**, 2286 (1997)
- 9 J. Liu, D. Kim, *IEEE J. Quantum Electron.* **QE-35**, 1724 (1999)
- 10 R.S. Conroy, C.F. Rae, G.J. Friel, M.H. Dunn, B.D. Sinclair, *Opt. Lett.* **23**, 1348 (1998)
- 11 Y.F. Chen, Y.C. Chen, S.W. Chen, Y.P. Lan, *Opt. Commun.* **234**, 337 (2004)
- 12 Y.F. Chen, S.W. Chen, L.Y. Tsai, Y.C. Chen, C.H. Chien, *Appl. Phys. B* **79**, 823 (2004)
- 13 K. Kato, *IEEE J. Quantum Electron.* **QE-27**, 1137 (1991)
- 14 A. Dubois, S. Victori, T. Lepine, P. Georges, A. Brun, *Appl. Phys. B* **67**, 181 (1998)
- 15 A. Agnesi, S. Dell'Acqua, C. Morello, G. Piccinno, G.C. Reali, Z. Sun, *IEEE J. Sel. Top. Quantum Electron.* **3**, 45 (1997)
- 16 Y.F. Chen, Y.P. Lan, H.L. Chang, *IEEE J. Quantum Electron.* **QE-37**, 462 (2001)
- 17 G. Xiao, M. Bass, M. Acharekar, *IEEE J. Quantum Electron.* **QE-34**, 2241 (1998)
- 18 W. Zendzian, J.K. Jabczynski, J. Kwiatkowski, *Appl. Phys. B* **76**, 355 (2003)
- 19 J.J. Degnan, *IEEE J. Quantum Electron.* **QE-25**, 214 (1989)